

Characterization of functionally significant coronary artery disease by a coronary computed tomography angiography-based index: a comparison with positron emission tomography

Constantinos D. Anagnostopoulos^{1*†}, Panagiotis K. Siogkas^{2,3†}, Riccardo Liga⁴, Georgios Benetos⁵, Teemu Maaniitty⁶, Antonis I. Sakellarios³, Iosif Koutagiar⁵, Ioannis Karakitsios¹, Michail I. Papafaklis⁷, Valentina Berti⁸, Roberto Sciagrà⁸, Arthur J.H.A. Scholte⁹, Lampros K. Michalis⁷, Oliver Gaemperli¹⁰, Philipp A. Kaufmann¹⁰, Gualtiero Pelosi⁴, Oberdan Parodi⁴, Juhani Knuuti⁶, Dimitrios I. Fotiadis^{2,3*‡}, and Danilo Neglia^{4,11‡}

¹Biomedical Research Foundation of Academy of Athens, 4 Soranou Efessiou, 11527 Athens, Greece; ²University of Ioannina, Materials Science and Engineering, Ioannina, Greece; ³Biomedical Research Institute, FORTH, Ioannina, Greece; ⁴Institute of Clinical Physiology, National Research Council, Pisa, IT, 56124, Italy; ⁵First Department of Cardiology, Hippokraton Hospital, National and Kapodistrian University Medical School, Athens, Greece; ⁶Turku PET Centre, Turku, Finland; ⁷University of Ioannina Medical School Ioannina, Greece; ⁸Department of Biomedical, Experimental and Clinical Sciences, Mario Serio, Nuclear Medicine Unit, University of Florence, Largo Brambilla 3, 50134 Florence, FI, Italy; ⁹Leiden University Medical Center, Leiden, Netherlands; ¹⁰University Hospital Zurich, Zurich, Switzerland; and ¹¹Fondazione Toscana Gabriele Monasterio, Pisa, IT, 56126, Italy

Received 18 July 2018; editorial decision 19 November 2018; accepted 19 December 2018

Aims

To test the hypothesis that virtual functional assessment index (vFAI) is related with regional flow parameters derived by quantitative positron emission tomography (PET) and can be used to assess abnormal vasodilating capability in coronary vessels with stenotic lesions at coronary computed tomography angiography (CCTA).

Methods and results

vFAI, stress myocardial blood flow (MBF), and myocardial flow reserve (MFR) were assessed in 78 patients (mean age 62.2 ± 7.7 years) with intermediate pre-test likelihood of coronary artery disease (CAD). Coronary stenoses ≥50% were considered angiographically significant. PET was considered positive for significant CAD, when more than one contiguous segments showed stress MBF ≤2.3 mL/g/min for ¹⁵O-water or <1.79 mL/g/min for ¹³N-ammonia. MFR thresholds were ≤2.5 and ≤2.0, respectively. vFAI was lower in vessels with abnormal stress MBF (0.76 ± 0.10 vs. 0.89 ± 0.07, *P* < 0.001) or MFR (0.80 ± 0.10 vs. 0.89 ± 0.07, *P* < 0.001). vFAI had an accuracy of 78.6% and 75% in unmasking abnormal stress MBF and MFR in ¹⁵O-water and 82.7% and 71.2% in ¹³N-ammonia studies, respectively. Addition of vFAI to anatomical CCTA data increased the ability for predicting abnormal stress MBF and MFR in ¹⁵O-water studies [AUC_{ccta+v fai} = 0.866, 95% confidence interval (CI) 0.783–0.949; *P* = 0.013 and AUC_{ccta+v fai} = 0.737, 95% CI 0.648–0.825; *P* = 0.007, respectively]. An incremental value was also demonstrated for prediction of stress MBF (AUC_{ccta+v fai} = 0.887, 95% CI 0.799–0.974; *P* = 0.001) in ¹³N-ammonia studies. A similar trend was recorded for MFR (AUC_{ccta+v fai} = 0.780, 95% CI 0.632–0.929; *P* = 0.13).

Conclusion

vFAI identifies accurately the presence of impaired vasodilating capability. In combination with anatomical data, vFAI enhances the diagnostic performance of CCTA.

* Corresponding author. Tel: +30 (210) 6597 126; Fax: +2106597490. E-mail: cdanagnostopoulos@bioacademy.gr; Tel: +30 (693) 2716 353. E-mail: fotiadis@cs.uoi.gr

† These authors are joint authors of this article.

‡ These authors are joint senior authors of this article.

Published on behalf of the European Society of Cardiology. All rights reserved. © The Author(s) 2019. For permissions, please email: journals.permissions@oup.com.

Keywords

computed tomography angiography • positron emission tomography • virtual functional assessment index • coronary artery disease • myocardial perfusion imaging • myocardial blood flow

Introduction

Coronary computed tomography angiography (CCTA) is the reference standard for non-invasive evaluation of coronary anatomy.¹ More recently, interrogation of functional significance of coronary lesions detected by CCTA has also become feasible through computation of computed tomography (CT)-derived fractional flow reserve (FFR_{CT}).² FFR_{CT} has demonstrated adequate accuracy for detection of haemodynamically significant lesions without additional radiation exposure³ and equivalent clinical outcomes, quality-of-life and lower costs, compared with usual care over 1-year follow-up.⁴ However, it has technical limitations⁵ and in addition, remote and lengthy core-laboratory analysis is required for the current version of the most commonly tested software.⁶ Virtual functional assessment index (vFAI) has been proposed⁷ as a computational FFR surrogate to detect flow-limiting coronary stenoses. This index can also be derived effectively from CCTA and an initial validation against invasive FFR has demonstrated good agreement between the two parameters.⁸

Coronary blood flow is a more comprehensive marker of the functional status of coronary circulation than pressure-derived estimates providing integrated assessment both of the epicardial vessels and the microcirculation, and therefore, constitutes a parameter of great interest for diagnostic and management strategies.⁹ In the non-invasive setting, quantitative measurement of myocardial blood flow (MBF) at rest and stress and myocardial flow reserve (MFR) using positron emission tomography (PET) provide accurate assessment of functionally significant coronary artery disease (CAD).¹⁰ A number of studies have explored the relationship between FFR, stress MBF, and MFR showing only a moderate correlation between those parameters.^{11–13} However, there are no studies testing the ability of CCTA-derived FFR to predict perfusion changes by PET downstream stenotic vessels. The purpose of the present study was to test the hypothesis that vFAI is related with regional flow parameters derived by quantitative PET and it can be used to detect impaired blood flow vasodilating capability in patients submitted to CCTA.

Methods

Study population

In the context of the FP-7 EVINCI (NCT00979199) and the Horizon 2020 SMARTool (www.smartool.eu) projects, individuals with stable symptoms and intermediate pre-test probability of CAD who, as per study protocol, have undergone both CCTA and PET perfusion with available quantitative data were identified. The time-interval between PET and CCTA studies was 6 ± 18 days. The characteristics of the study population, details on imaging procedures and protocols have already been described elsewhere.¹⁴ Based on the selection criteria for the SMARTool project, only EVINCI studies with a fair to excellent CCTA image quality were included in the analysis. Accordingly, 21 from the 99

EVINCI patients who have undergone both CCTA and PET were excluded, as they did not meet the pre-specified standards. The included patients had at least one vessel free of noise, motion artefacts, or heavy calcifications and a maximum increment between slices of less or equal to 0.625 mm.

CCTA imaging and processing

The CCTA acquisition protocol ([Supplementary data online](#)) has been described in detail previously.¹⁴ Scan quality of the CCTA was classified as excellent, good, fair, and poor.

3D reconstruction process

The 3D reconstruction was performed using in-house developed algorithms and the reconstruction process was carried out as previously described.⁷ It is carried out in seven steps as follows: (i) pre-processing of the CCTA images with the Frangi Vesselness filter is performed limiting the region of interest to possible vessel regions; (ii) using a minimum cost path approach, the 3D centreline of the vessels is then extracted; (iii) employing a membership function of Hounsfield Units (HU) values and the distance from the centreline, an estimation of the weight function for lumen, outer wall, and calcified plaque is made. An extension of the active contour model estimation for (iv) the lumen and (v) the outer wall segmentation are subsequently implemented; (vi) regarding plaque segmentation, a level set method is applied, taking into account calcified objects of significant size; (vii) finally, the 3D surfaces for the lumen, outer wall, and calcified plaques are created. For the purpose of the present study only main coronary branches were used for analysis. Accordingly, for right coronary artery (RCA) vessels, segments 1–3 were included in the reconstruction process, for left anterior descending artery (LAD), segments 6–8, and for the left circumflex artery (LCx), segments 11 and 13 were included, according to the SYNTAX SCORE mapping.

vFAI calculation

Blood flow simulations were carried out using a finite element commercial software (ANSYS® CFX 15, Canonsburg, PA, USA). A tetrahedral mesh was created for each vessel and the Navier–Stokes and continuity equations were solved. The vFAI calculation process has been described in detail in Ref.⁷ Briefly, the aforementioned blood flow simulations are performed to calculate the ratio of distal to proximal pressure over the examined segment for volumetric flows in the range from 0 mL/s to 4 mL/s, normalized by the ratio over this range for a completely healthy arterial segment, offering a measure of haemodynamic significance that is numerically equivalent to the average of the computed pressure ratio over this flow range. vFAI computation was performed by a reader with experience in analysing CCTA images and using the 3D reconstruction module optimally, who was unaware of the perfusion and hybrid CCTA-PET results. Specific procedural details are described in vFAI calculation ([Supplementary data online](#)).

PET imaging and data analysis

PET scanning with ¹⁵O-water or ¹³N-ammonia was performed according to international guidelines as described elsewhere.¹⁵ Protocol details are described in PET imaging ([Supplementary data online](#)). CCTA and PET images were fused to assign each myocardial segment to the pertinent coronary territory and every coronary stenosis to areas of myocardial

Table 1 Baseline patient characteristics

Patients (n = 78)	N (%)
Age (years)	62.2 ± 7.7
Gender (male)	38 (54)
Symptoms	
Typical angina	11 (15)
Atypical angina	42 (60)
Non-anginal chest pain	18 (25)
Risk factors	
Arterial hypertension	37 (52)
Dyslipidaemia	43 (61)
Smoking	14 (20)
Family history of CAD	26 (37)
Diabetes mellitus	11 (15)
Obesity	13 (18)
BMI	26.9 ± 3.7
Medications	
Oral antidiabetics	8 (11)
Insulin	4 (6)
Statins	42 (59)
ACEI	22 (31)
Diuretics	10 (14)
ARBs	11 (15)
β-blockers	39 (55)
Calcium antagonists	9 (13)
ASA	53 (75)
Nitrates	9 (13)
Total vessels analysed (vFAI)	212
LAD	75 (35.4)
RCA	74 (34.9)
LCx	63 (29.7)
Total vessels with stenosis ≥50% (vFAI)	45
¹⁵ O-water	31 (19.5)
¹³ N-ammonia	14 (26.4)
LVEF	54.94 ± 7.05

ACEI, angiotensin-converting-enzyme inhibitor; ARBs, angiotensin II receptor blockers; ASA, aspirin; BMI, body mass index; CAD, coronary artery disease; LAD, left anterior descending artery; LCx, left circumflex artery; LVEF, left ventricular ejection fraction; RCA, right coronary artery; vFAI, virtual functional assessment index.

perfusion using a dedicated workstation (Advantage Workstation 4.4, GE Healthcare) and the CardIQ Fusion software package (GE Healthcare) as previously described.¹⁶ Accordingly, to define accurately the functional significance of coronary stenoses, the specific myocardial segments distal to the pertinent coronary lesions were identified and the respective MBF averaged. PET flow quantitation and selection of thresholds in flow values for detection of significant CAD was performed as previously reported. Specifically, PET studies were considered positive for impaired coronary blood flow, when more than one contiguous segments showed stress MBF ≤ 2.3 mL/g/min for ¹⁵O-water or < 1.79 mL/g/min for ¹³N-ammonia.^{15,17} The corresponding MFR thresholds were ≤ 2.5 and ≤ 2 for ¹⁵O-water and ¹³N-ammonia, respectively.^{15,17} Analysis of all PET images was performed by two experienced independent physicians who were unaware of the patients' data.

Statistical analysis

Quantitative data are presented as mean values ± SD, while qualitative variables as absolute and relative frequencies. Probability values are two-sided from the Student's *t*-test or the Mann–Whitney *U* test for continuous variables, according to the normal or skewed distribution of the variables. Assessment for normality of data distribution was evaluated by Kolmogorov–Smirnov test. For multiple groups comparisons, ANOVA or Kruskal–Wallis test was used. A *P*-value < 0.05 was considered statistically significant. To assess the relationship between CCTA-vFAI values and PET-derived parameters, the Pearson's correlation coefficient was used. The optimal threshold of vFAI for predicting an attenuated response to pharmacological stress in PET ¹⁵O-water or ¹³N-ammonia studies was determined using the Youden index. Subsequently for identifying a single cut-off, potential statistically significant differences in diagnostic performance between the latter and individual tracer and PET index (stress MBF or MFR)-specific thresholds were assessed by comparison of the receiver operator characteristics (ROC) curves with the DeLong method. The level of agreement between stress MBF or MFR and vFAI was assessed by Cohen's κ -statistic.

Angiographic stenosis severity was classified as: $< 30\%$, 30–49%, 50–70%, and 70–90%. A threshold of a stenosis severity $\geq 50\%$ on CCTA was used for defining angiographically significant coronary stenosis. When multiple stenoses were present in the same vessel, the most severe one was used to assess the CCTA performance for detecting impaired stress MBF or MFR. Sensitivity and specificity values of CCTA and vFAI for identification of abnormal hyperaemic response or MFR were calculated. The following models were constructed and compared using Harrel's *c*-statistics: CCTA (using as cut-off $\geq 50\%$), vFAI (as dichotomous variable, normal–abnormal) and vFAI + CCTA (computed by means of logistic regression model).¹⁸ Statistical analyses were performed using the SPSS software version 20 (Chicago, IL, USA), while MedCalc software version 13 (Ostend, Belgium) was used for the comparison of the areas under the ROC curves.¹⁹

Results

Patient and vessel characteristics

Baseline demographic, clinical, and lesion characteristics of the study population are summarized in *Table 1*. By hybrid imaging analysis, from a total of 234 coronary arteries, in 22 vessels vFAI was not performed because either of sub-optimal image quality (3 LAD, 4 LCx, and 3 RCA), or having limited contribution to the perfusion of the corresponding myocardial territory (12 RCA). From the remaining 212 vessels, in which vFAI was calculated, 61, 39, and 6 coronary arteries had a 30–49% (57.0%), 50–70% (36.4%), and 70–90% stenosis (5.6%) on CCTA, respectively. Eighteen vessels with a stenosis $\geq 30\%$ presented multiple lesions (16.8%). MBF and MFR values were quantitated by ¹³N-ammonia for 53 vessels (14 with $\geq 50\%$ stenosis) and by ¹⁵O-water for 159 vessels (31 with $\geq 50\%$ stenosis).

Impact of stenosis severity on quantitative coronary functional parameters

vFAI values corresponding to lesions $\geq 50\%$ were significantly lower compared with those of intermediate severity (30–49%) and non-stenotic lesions ($< 30\%$). Similarly, stress MBF and MFR values derived

from ^{15}O -water PET studies declined significantly downstream stenotic coronary arteries as compared to vessels with <30% stenosis. The same trend was shown for ^{13}N -ammonia studies even if the differences did not reach statistical significance (Table 2).

Table 2 Impact of stenosis severity on quantitative coronary functional parameters

	Stenosis severity			P-value
	<30% (n = 81)	30–50% (n = 47)	>50% (n = 31)	
^{15}O -water				
vFAI ^a	0.91 ± 0.06	0.84 ± 0.09	0.78 ± 0.12	<0.001
Stress MBF	3.66 ± 0.90 ^{b,c}	3.08 ± 0.98 ^b	2.55 ± 1.25 ^c	<0.001
MFR ^d	3.25 ± 1.04	2.70 ± 0.79	2.12 ± 0.72	<0.001
^{13}N -ammonia				
vFAI	0.92 ± 0.05 ^{e,f}	0.84 ± 0.06 ^f	0.81 ± 0.07 ^e	<0.001
Stress MBF	2.38 ± 0.49	2.27 ± 0.57	1.99 ± 0.68	0.12
MFR	2.70 ± 0.80	2.56 ± 0.63	2.11 ± 0.80	0.08
Both tracers				
vFAI ^g	0.91 ± 0.06	0.84 ± 0.08	0.79 ± 0.10	<0.001

MFR, myocardial flow reserve; vFAI, virtual functional assessment index.

^a $P < 0.05$ for all between group comparisons.

^{b,c} $P < 0.05$ for between group comparisons.

^d $P < 0.05$ for all between group comparisons.

^{e,f} $P < 0.05$ for between group comparisons.

^g $P < 0.05$ for all between group comparisons.

Relationship between vFAI and PET parameters

Figure 1 demonstrates the relationship between vFAI and PET-derived indices. vFAI was positively correlated with stress MBF ($R = 0.49$, $P < 0.001$ and $R = 0.53$, $P = 0.001$) for ^{15}O -water and ^{13}N -ammonia-based measurements, respectively (Figure 1A and B). A positive correlation was also demonstrated between vFAI and MFR ($R = 0.41$, $P < 0.001$ and $R = 0.39$, $P = 0.004$) for ^{15}O -water and ^{13}N -ammonia-based measurements, respectively (Figure 1C and D).

In analysis of all 212 vessels, vFAI was lower in vessels with abnormal stress MBF (median 0.79, P25–P75: 0.68–0.83 vs. median 0.90, P25–P75 0.86–0.93, $P < 0.001$, Figure 2A). Similarly, vFAI was lower in vessels with abnormal MFR (median 0.82, P25–P75: 0.76–0.89 vs. 0.91, P25–P75: 0.86–0.94, $P < 0.001$, Figure 2B).

Performance of vFAI for predicting reduced hyperaemic response or MFR

For ^{15}O -water PET studies, a vFAI threshold ≤ 0.8 [AUC: 0.856, 95% confidence interval (CI) 0.775–0.938; $P < 0.001$] had a per-vessel sensitivity and specificity, of 77.8% and 90.9%, respectively, for predicting a stress MBF ≤ 2.3 (Figure 3A). For identifying an MFR ≤ 2.5 , the corresponding values for a vFAI threshold ≤ 0.86 (AUC: 0.796, 95% CI 0.724–0.868; $P < 0.001$) were 66.7% and 79%, respectively (Figure 3B). A threshold of ≤ 0.8 had sensitivity 84% and specificity 91% (AUC 0.899, 95% CI 0.836–0.961;

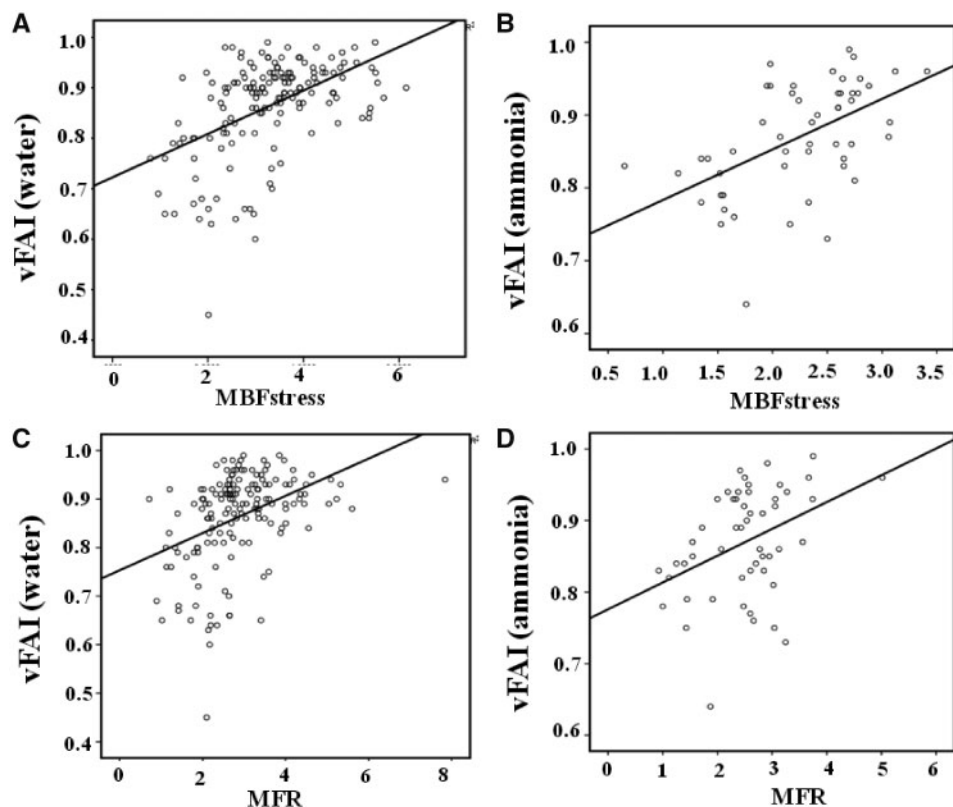


Figure 1 Scatterplots showing Pearson's correlation between vFAI and ^{15}O -water PET stress MBF (A) and MFR (C), as well as between vFAI and ^{13}N -ammonia stress MBF (B) and MFR, respectively (D). All quantitative ^{15}O -water and ^{13}N -ammonia indices associated significantly with vFAI.

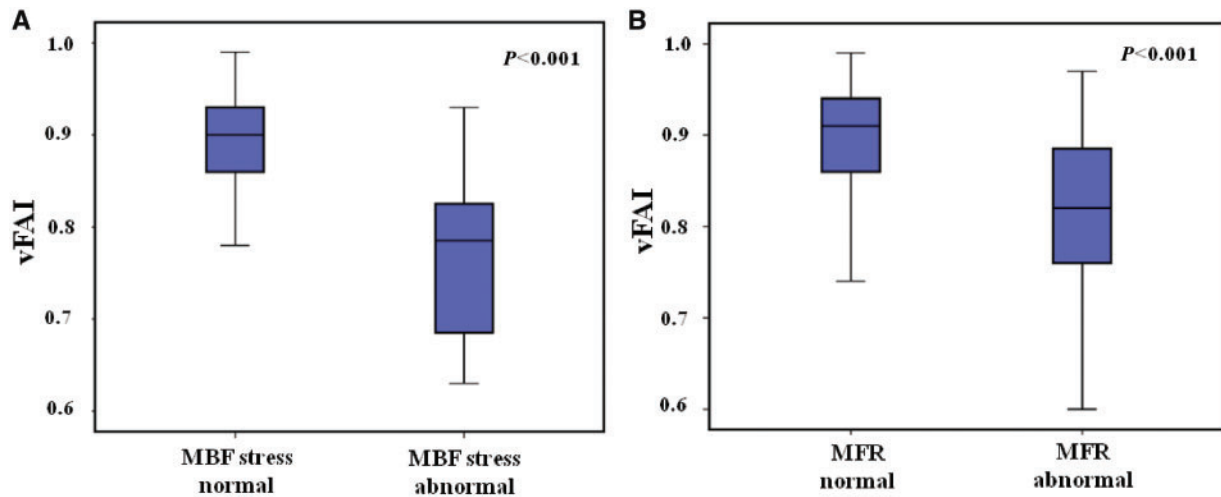


Figure 2 vFAI in normal vs. abnormal stress MBF and MFR territories. vFAI was significantly lower in vessels with abnormal stress MBF (A) or MFR (B).

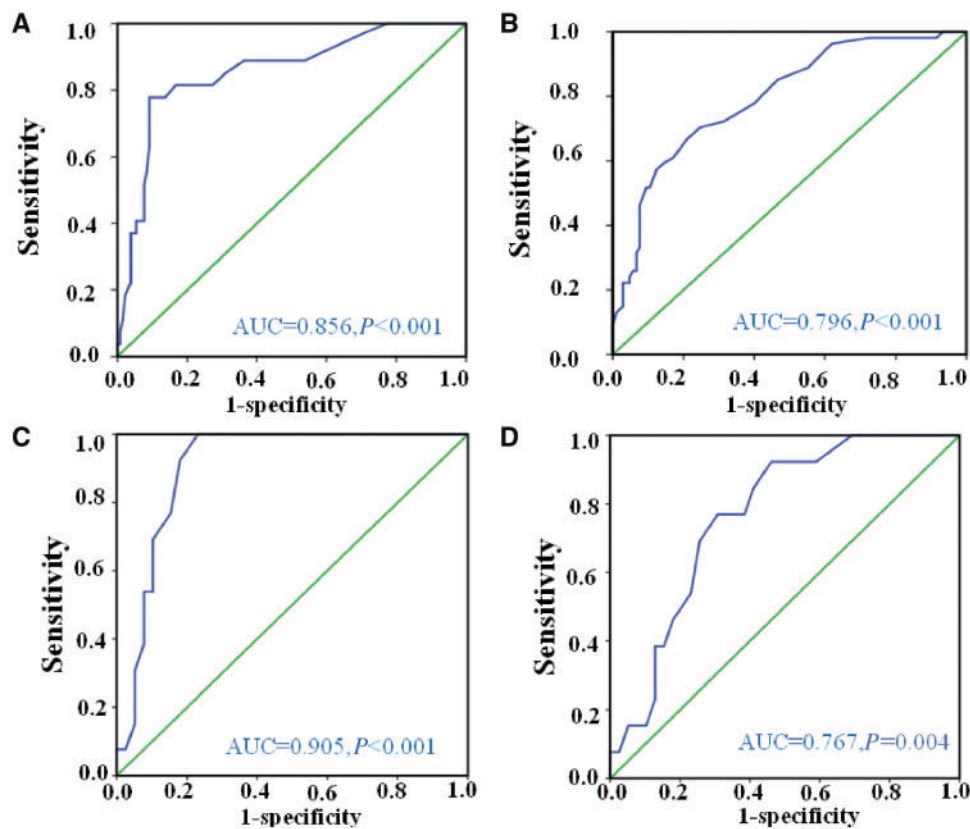


Figure 3 ROC curves of the diagnostic performance of vFAI for detecting attenuated stress MBF ≤ 2.3 (A) or MFR ≤ 2.5 (B) for ^{15}O -water PET studies, and stress MBF < 1.79 (C) or MFR < 2 (D) for ^{13}N -ammonia studies.

$P < 0.001$) for predicting concordant impairment of both stress MBF and MFR. For ^{13}N -ammonia, the optimal threshold of vFAI to detect a stress MBF < 1.79 was ≤ 0.85 (AUC: 0.905, 95% CI 0.825–0.986; $P < 0.001$); per-vessel sensitivity 100%, specificity, 76.9%.

The same threshold could predict an abnormal MFR < 2 with sensitivity 76.9% and specificity 69.2% (AUC: 0.767, 95% CI 0.635–0.899; $P = 0.004$) (Figure 3C and D). A vFAI ≤ 0.85 (AUC 0.856, 95% CI 0.756–0.956; $P = 0.001$) had sensitivity 100% and specificity

Table 3 Diagnostic performance of vFAI with a cut-off ≤ 0.85 in predicting an abnormal stress MBF or MFR

	ROC cut-off (%)	Cut-off: 0.85 (%)	P-value
¹⁵O-water			
Stress MBF			
Sensitivity	77.8	81.5	0.0519
Specificity	90.9	78	
MFR			
Sensitivity	66.7	61.1	0.6337
Specificity	77.9	82.9	
¹³N-ammonia			
Stress MBF			
Sensitivity		100	
Specificity		76.9	
MFR			
Sensitivity		76.9	
Specificity		69.2	

71.4% for predicting concordant impairment of both stress MBF and MFR.

Considering the propinquity of these cut-off values, the diagnostic accuracy of a single vFAI threshold 0.85 was tested against the tracer-specific individual threshold values. No statistically significant differences in diagnostic performance were identified and for practical purposes, a single threshold of ≤ 0.85 was used for subsequent analysis. vFAI had an accuracy of 78.6% and 75% in unmasking abnormal stress MBF and MFR in ¹⁵O-water and 82.7% and 71.2% in ¹³N-ammonia studies, respectively. Details of diagnostic characteristics of vFAI for predicting impaired coronary vasodilating response with a cut-off value ≤ 0.85 vs. the optimal cut-offs are presented in Table 3. Agreement between vFAI and PET measurements is shown in Supplementary data online, Table S1.

Comparison of CCTA and vFAI for predicting reduced hyperaemic response or MFR

The rates of territories with normal vs. abnormal stress MBF or MFR in relation to stenosis severity and vFAI, for the total analysed vessels are presented in Figure 4.

Sensitivity and specificity of CCTA for detecting an abnormal stress MBF in ¹⁵O-water studies, using as threshold a stenosis severity $\geq 50\%$ were 63% and 89.4% whilst, the corresponding values for predicting an attenuated MFR were 35.2% and 88.6%, respectively. Sensitivity and specificity of CCTA for detecting an abnormal stress MBF in ¹³N-ammonia studies were 42.9% and 73.8% whilst, the corresponding values for predicting an attenuated MFR were 53.3% and 78%, respectively.

The performance of vFAI for predicting abnormal stress MBF in ¹⁵O-water studies was similar to that of CCTA ($AUC_{v\text{fai}} = 0.798$, 95% CI 0.703–0.892 vs. $AUC_{\text{ccta}} = 0.762$, 95% CI 0.648–0.876; $P = 0.54$, respectively). However, the addition of vFAI variable to CCTA, increased the predictive ability of the anatomy-based model significantly ($AUC_{\text{ccta} + \text{v\text{fai}}} = 0.866$, 95% CI 0.783–0.949; $P = 0.013$).

vFAI performed better than CCTA for predicting abnormal MFR ($AUC_{v\text{fai}} = 0.720$, 95% CI 0.631–0.808 and $AUC_{\text{ccta}} = 0.619$, 95% CI 0.523–0.715; $P = 0.02$). Moreover, the addition of vFAI variable to CCTA increased the predictive capacity of the anatomy-based model significantly ($AUC_{\text{ccta} + \text{v\text{fai}}} = 0.737$, 95% CI 0.648–0.825; $P = 0.007$).

vFAI performed better than CCTA for predicting abnormal stress MBF in ¹³N-ammonia studies ($AUC_{v\text{fai}} = 0.885$, 95% CI 0.796–0.973 and $AUC_{\text{ccta}} = 0.628$, 0.444–0.813; $P = 0.002$). Moreover, the addition of vFAI variable to CCTA increased the predictive capacity of the model significantly ($AUC_{\text{ccta} + \text{v\text{fai}}} = 0.887$, 95% CI 0.799–0.974; $P = 0.001$). There was no significant difference between the model based on CCTA and the model based on vFAI for prediction of abnormal MFR ($AUC_{v\text{fai}} = 0.731$, 95% CI 0.572–0.889 and $AUC_{\text{ccta}} = 0.679$, 95% CI 0.499–0.860; $P = 0.58$). The addition of vFAI to the model based on CCTA demonstrated the same trend as in the ¹⁵O-water studies, even if it did not reach statistical significance ($AUC_{\text{ccta} + \text{v\text{fai}}} = 0.780$, 95% CI 0.632–0.929; $P = 0.13$).

An example of a patient with multiple vessel CAD, abnormal vFAI and MFR in the corresponding coronary territories is shown in Figure 5.

Discussion

Our main results can be summarized as follows: vFAI (i) can be readily computed from standard CCTA datasets, (ii) correlates modestly with stress MBF and MFR, (iii) performs well in identifying coronary lesions with downstream impairment of stress MBF or MFR, and (iv) in combination with anatomical data enhances the diagnostic performance of CCTA.

Stenosis severity vs. functional indices

Our study is the first to test the relationship between CCTA stenosis severity, CCTA-based estimates of FFR and specific MBF calculation. We demonstrated that vFAI was lower in vessels with stenotic lesions compared with those without stenosis and those vessels with lesions $\geq 50\%$ had lower vFAI values compared with those with 30–49% stenosis. PET measurements demonstrated a similar pattern of impaired coronary vasodilating capability in relation to stenosis severity. In ¹⁵O-water PET studies, the decline of stress MBF and MFR in stenotic coronary arteries compared with vessels with $< 30\%$ stenosis was more significant than in ¹³N-ammonia studies. This difference could be explained by the small number of vessels with higher stenosis grade ($> 70\%$) in the present series. Differences between tracers in terms of extraction fraction and modelling approaches for perfusion quantification may have increased the accuracy of ¹⁵O-water based measurements in this population.

Pressure-based measurements vs. quantitative myocardial perfusion

Pressure-derived measures of CAD haemodynamic significance (i.e. FFR and FFR_{CT}) can only give an indirect assessment of coronary flow capacity, showing a frequent discrepancy with MFR.^{20–22} In keeping with these observations, we have demonstrated that although vFAI was significantly lower in vessels with abnormal stress MBF or MFR, overall, there was a rather weak to modest correlation between vFAI and these two parameters and a poor to fair

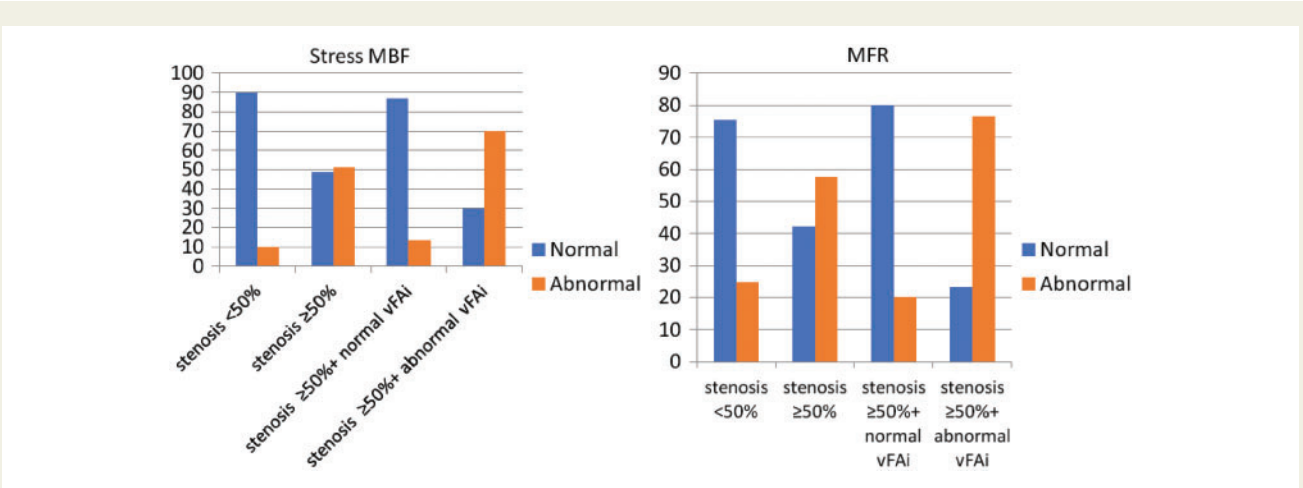


Figure 4 Rates of territories with normal vs. abnormal stress MBF or MFR in relation to stenosis severity and vFAI.

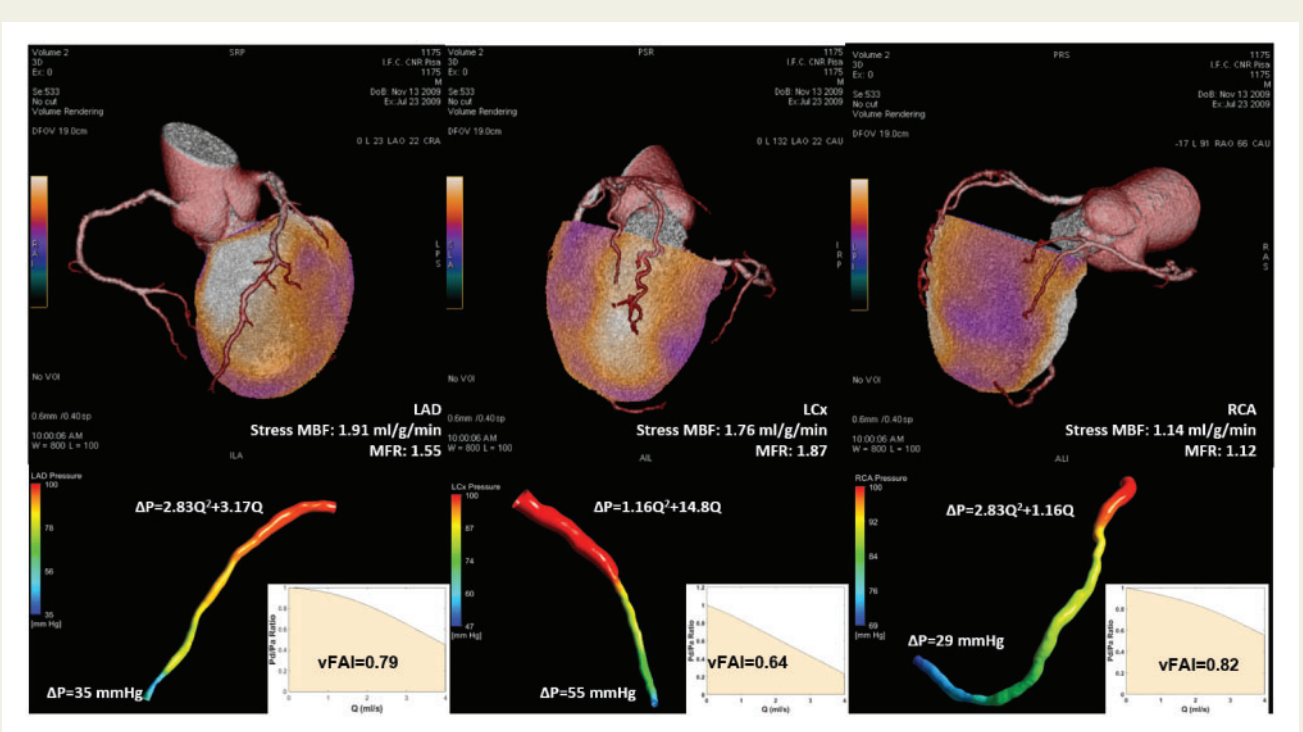


Figure 5 A 74-year-old man with typical angina and evidence of triple vessel CAD with 50–70% stenoses in the distal LAD, second obtuse marginal branch, and proximal RCA at CCTA. Hybrid PET/CCTA imaging with ¹³N-ammonia showed impaired coronary flow capacity in all territories colocalized with the stenosed coronary vessels (upper panels). vFAI was also reduced in all three coronary vessels (lower panels). The middle panel depicts the pressure distribution for a flow of 3 mL/s, along with the final P_d/P_a equation for each vessel.

agreement, with κ values ranging from 0.38 to 0.63. Possible explanations are either the generalizations used for computation of vFAI (i.e. rest and stress coronary flow equalled to 1 mL/s and 3 mL/s, respectively) or the physiological and technical determinants of absolute flow and flow reserve measurements by PET.²¹ Like FFR, vFAI can be reduced in cases of epicardial disease, but MFR can be preserved, if there is an intact vasodilator response.²⁰ Conversely, impaired MFR with a normal vFAI may be the result of microvascular dysfunction

alone or in combination with an anatomically unobstructed coronary artery. In our study, impaired stress MBF or MFR was present in 10.2% and 24.7% of vessels with anatomical stenosis <50%, respectively. Finally, since only main coronary branches were considered for the analysis, the possible confounding role on myocardial perfusion of coronary lesions located in minor-branches cannot be excluded as a cause of the rather modest concordance between vFAI and PET measurements.

Prediction of attenuated hyperaemic response or MFR

We found that vFAI performs well in identifying coronary lesions with downstream impairment of stress MBF or MFR. The present study is the first to demonstrate the value of CCTA-based estimates of FFR in predicting coronary flow capacity on PET imaging, adding also incremental value over CCTA anatomical data. Our threshold is different to that of FFR_{CT} , since there are important methodological differences between assessment of the latter and vFAI, which in contrast to FFR_{CT} reflects only vessel geometry-related changes, without taking into account alterations at the microcirculation level or vascular resistance and their influence in coronary flow during hyperaemia. Moreover, the optimal threshold of vFAI for detecting impaired coronary blood flow vasodilating capability by PET is somewhat higher than that previously reported by our group (≤ 0.82) using FFR as the gold standard,⁸ probably as a result of intrinsic differences between the two gold-standards for evaluation of the functional significance of a coronary lesion.

Clinical implications

The development of a CCTA-based index, which could detect reliably the functional significance of a coronary lesion in the range of 30–90% has become of paramount importance as it will allow a complete anatomical-functional characterization of CAD burden by a single investigation, possibly reducing the downstream inappropriate referral to invasive coronary angiography.²³ In this context, vFAI is a validated index of CAD haemodynamic significance, derived from the application of computational flow dynamics to standard CCTA datasets, without need for extra radiation exposure. Its main advantage is the evidently shorter required computational time to obtain the results of each case.⁸ As reported recently, the mean analysis time required for each of the assessed arteries was 25 ± 10 min, with an average 3D reconstruction time of around 3 min.⁸ Furthermore, in contrast to FFR_{CT} , which requires core-laboratory analysis, vFAI can be directly calculated from a simple personal computer. Interestingly, while CT-based FFR has already been shown to mimic the results of invasive FFR,^{24–26} a validation against PET-derived absolute MBF measurements as integrated measures of global coronary fluid dynamics, has never been performed. This aspect is of particular relevance, since vFAI, obtained after the 3D modelling of coronary plaque burden, may only simulate the haemodynamic impact of epicardial atherosclerosis, disregarding the possible impact of underlying microvascular dysfunction or vascular resistance. Despite these intrinsic methodological particularities, our results indicate that vFAI might be an appropriate tool for interrogating the functional significance of a coronary stenosis at CCTA and they could also suggest a possible role of vFAI as a gatekeeper to invasive coronary angiography.

Limitations

The results of the present study should be interpreted by taking into account its rather modest sample size and small number of vessels with stenosis severity $>70\%$. Therefore, we have performed only a per-vessel evaluation of CCTA and corresponding PET data analysis. On the other hand, we have studied only patients with intermediate likelihood of CAD and followed a hybrid imaging-based approach of CCTA and PET datasets achieving optimal co-localization of each

coronary artery with the pertinent myocardial territory, thus avoiding any incorrect assignment of vFAI and MBF data. vFAI was calculated only in the major coronary segments (i.e. 1–3, 6–8, and 11 and 13, in accordance with the SYNTAX SCORE mapping). We have excluded a number of patients from the initial cohort, because of significant motion or calcification in CCTA, factors that hamper image quality and vFAI assessment; however, this is within the range reported previously.²⁷ In our study, the degree of anatomic stenosis was derived from CCTA and not from coronary angiography, which is the gold standard for narrowing assessment. Nonetheless, the excellent accuracy of CCTA in quantifying CAD severity has already been demonstrated, making this non-invasive technique of particular value in the evaluation of patients with an intermediate pre-test probability of CAD.¹⁴ The fact that in patients with multiple significant coronary stenoses in series only the most severe lesion was used for testing CCTA performance might have added a possible limitation to data analysis. However, since only a minor proportion of vessels (6%) had lesions greater than 50% and multiple stenoses, it is rather unlikely that they could have affected significantly our results. We acknowledge that from the current dataset, we cannot identify on an individual basis, patients who will not need further functional testing. However, this was not the aim of the current study and needs to be assessed in larger prospective multicentre studies.

Conclusions

Computation of vFAI from CCTA datasets is feasible and is significantly correlated with PET measured stress MBF and MFR. vFAI defines with reasonable accuracy the presence of haemodynamically significant CAD, likely representing a valid additional tool for comprehensive anatomical-functional characterization of CAD by CCTA.

Supplementary data

Supplementary data are available at *European Heart Journal - Cardiovascular Imaging* online.

Funding

This project has received funding from the European Union's Horizon 2020 research and innovation programme under grant agreement No 68906. This article reflects only the authors view. The Commission is not responsible for any use that may be made of the information it contains. This work has also been partly funded by I.K.Y. (State Scholarships Foundation) scholarship, which was funded by the Act 'Support of Postdoctoral Researchers' from funds of Research Programme 'Development of Human Resource, Education and Continued Learning', with priority bases 6,8,9 and cofunded by the European Social Fund (ESF) and the Greek State.

Conflict of interest: none declared.

References

- Montalescot G, Sechtem U, Achenbach S, Andreotti F, Arden C, Budaj A et al. 2013 ESC guidelines on the management of stable coronary artery disease: the Task Force on the management of stable coronary artery disease of the European Society of Cardiology. *Eur Heart J* 2013;**34**:2949–3003.
- Schuijff JD, Ko BS, Di Carli MF, Hislop-Jambrich J, Ihdahid AR, Seneviratne SK et al. Fractional flow reserve and myocardial perfusion by computed tomography: a guide to clinical application. *Eur Heart J Cardiovasc Imaging* 2018;**19**:127–35.

3. Min JK, Leipsic J, Pencina MJ, Berman DS, Koo BK, van Mieghem A *et al.* Diagnostic accuracy of fractional flow reserve from anatomic CT angiography. *JAMA* 2012;**308**:1237–45.
4. Douglas PS, De Bruyne B, Pontone G, Patel MR, Norgaard BL, Byrne RA *et al.* 1-year outcomes of FFR_{CT}-guided care in patients with suspected coronary disease: the PLATFORM study. *J Am Coll Cardiol* 2016;**68**:435–45.
5. Tesche C, De Cecco CN, Albrecht MH, Duguay TM, Bayer RR, Litwin SE *et al.* Coronary CT angiography-derived fractional flow reserve. *Radiology* 2017;**285**:17–33.
6. Koo BK, Erglis A, Doh JH, Daniels DV, Jegere S, Kim HS *et al.* Diagnosis of ischemia-causing coronary stenoses by noninvasive fractional flow reserve computed from coronary computed tomographic angiograms. Results from the prospective multicenter DISCOVER-FLOW (Diagnosis of Ischemia-Causing Stenoses Obtained Via Noninvasive Fractional Flow Reserve) study. *J Am Coll Cardiol* 2011;**58**:1989–97.
7. Papafaklis MI, Muramatsu T, Ishibashi Y, Lakkas LS, Nakatani S, Bourantas CV *et al.* Fast virtual functional assessment of intermediate coronary lesions using routine angiographic data and blood flow simulation in humans: comparison with pressure wire—fractional flow reserve. *EuroIntervention* 2014;**10**:574–83.
8. Siogkas PK, Anagnostopoulos CD, Liga R, Exarchos TP, Sakellarios AI, Rigas G *et al.* Noninvasive CT-based hemodynamic assessment of coronary lesions derived from fast computational analysis: a comparison against fractional flow reserve. *Eur Radiol* 2018; doi:10.1007/s00330-018-5781-8.
9. van de Hoef TP, Siebes M, Spaan JA, Piek JJ. Fundamentals in clinical coronary physiology: why coronary flow is more important than coronary pressure. *Eur Heart J* 2015;**36**:3312–19a.
10. Taqueti VR, Di Carli MF. Clinical significance of noninvasive coronary flow reserve assessment in patients with ischemic heart disease. *Curr Opin Cardiol* 2016; **31**:662–9.
11. van de Hoef TP, van Lavieren MA, Damman P, Delewi R, Piek MA, Chamuleau SA *et al.* Physiological basis and long-term clinical outcome of discordance between fractional flow reserve and coronary flow velocity reserve in coronary stenoses of intermediate severity. *Circ Cardiovasc Interv* 2014;**7**:301–11.
12. Echavarría-Pinto M, Escaned J, Macías M, Medina M, Gonzalo N, Petraco R *et al.* Disturbed coronary hemodynamics in vessels with intermediate stenoses evaluated with fractional flow reserve: a combined analysis of epicardial and microcirculatory involvement in ischemic heart disease. *Circulation* 2013;**128**:2557–66.
13. Danad I, Szymonifka J, Schulman-Marcus J, Min JK. Static and dynamic assessment of myocardial perfusion by computed tomography. *Eur Heart J Cardiovasc Imaging* 2016;**17**:836–44.
14. Neglia D, Rovai D, Caselli C, Pietila M, Teresinska A, Aguadé-Bruix S *et al.* Detection of significant coronary artery disease by noninvasive anatomical and functional imaging. *Circ Cardiovasc Imaging* 2015;**8**. pii:002179. doi:10.1161/CIRCIMAGING.114.002179.
15. Berti V, Sciagra R, Neglia D, Pietilä M, Scholte AJ, Nekolla S *et al.* Segmental quantitative myocardial perfusion with PET for the detection of significant coronary artery disease in patients with stable angina. *Eur J Nucl Med Mol Imaging* 2016; **43**:1522–9.
16. Liga R, Vontobel J, Rovai D, Marinelli M, Caselli C, Pietila M *et al.* Multicentre multi-device hybrid imaging study of coronary artery disease: results from the Evaluation of INtegrated Cardiac Imaging for the Detection and Characterization of Ischaemic Heart Disease (EVINCI) hybrid imaging population. *Eur Heart J Cardiovasc Imaging* 2016;**17**:951–60.
17. Danad I, Uusitalo V, Kero T, Saraste A, Rajmakers PG, Lammertsma AA *et al.* Quantitative assessment of myocardial perfusion in the detection of significant coronary artery disease: cutoff values and diagnostic accuracy of quantitative [(15)O]H₂O PET imaging. *J Am Coll Cardiol* 2014;**64**:1464–75.
18. Harrell FE Jr, Califf RM, Pryor DB, Lee KL, Rosati RA. Evaluating the yield of medical tests *JAMA* 1982;**247**:2543–46.
19. DeLong ER, DeLong DM, Clarke-Pearson DL. Comparing the areas under two or more correlated receiver operating characteristic curves: a nonparametric approach. *Biometrics* 1988;**44**:837–45.
20. Zimmermann FM, Pijls NHJ, De Bruyne B, Bech GJ, van Schaardenburgh P, Kirkeeide RL *et al.* What can intracoronary pressure measurements tell us about flow reserve? Pressure-bounded coronary flow reserve and example application to the randomized DEFER trial. *Catheter Cardiovasc Interv* 2017;**90**:917–25.
21. Gould KL, Johnson NP, Bateman TM, Beanlands RS, Bengel FM, Bober R *et al.* Anatomic versus physiologic assessment of coronary artery disease. Role of coronary flow reserve, fractional flow reserve, and positron emission tomography imaging in revascularization decision-making. *J Am Coll Cardiol* 2013;**62**:1639–53.
22. Johnson NP, Kirkeeide RL, Gould KL. Is discordance of coronary flow reserve and fractional flow reserve due to methodology or clinically relevant coronary pathophysiology? *JACC Cardiovasc Imaging* 2012;**5**:193–202.
23. Curzen NP, Nolan J, Zaman AG, Nørgaard BL, Rajani R. Does the routine availability of CT-derived FFR influence management of patients with stable chest pain compared to CT angiography alone?: the FFRCT RIPCORDER Study. *JACC Cardiovasc Imaging* 2016;**9**:1188–94.
24. Gonzalez JA, Lipinski MJ, Flors L, Shaw PW, Kramer CM, Salerno M. Meta-analysis of diagnostic performance of coronary computed tomography angiography, computed tomography perfusion, and computed tomography-fractional flow reserve in functional myocardial ischemia assessment versus invasive fractional flow reserve. *Am J Cardiol* 2015;**116**:1469–78.
25. Nakanishi R, Osawa K, Ceponiene I, Huth G, Cole J, Kim M *et al.* The diagnostic performance of SPECT-MPI to predict functional significant coronary artery disease by fractional flow reserve derived from CCTA (FFRCT): sub-analysis from ACCURACY and VCT001 studies. *Int J Cardiovasc Imaging* 2017;**33**:2067–72.
26. Nakazato R, Park HB, Berman DS, Gransar H, Koo BK, Erglis A *et al.* Noninvasive fractional flow reserve derived from computed tomography angiography for coronary lesions of intermediate stenosis severity: results from the DeFACTO study. *Circ Cardiovasc Imaging* 2013;**6**:881–9.
27. Kruk M, Wardziak Ł, Demkow M, Pleban W, Pręgowski J, Dzielińska Z *et al.* Workstation-based calculation of CTA based FFR for intermediate stenosis. *JACC Cardiovasc Imaging* 2016;**9**:690–9.